PICO: Probe of Inflation and Cosmic Origins

Thematic Area: Space Based Projects

Lead Author: Shaul Hanany (hanany@umn.edu) [1]

Authors

Marcelo Alvarez [9,16]
Emmanuel Artis [12]
Peter Ashton [24,16,9]
Jonathan Aumont [25]
Ragnhild Aurlien [26]
Ranajoy Banerji [26]
R. Belen Barreiro [27]
James G. Bartlett [5,6]
Soumen Basak [28]
Nick Battaglia [7]
Jamie Bock [8,6]
Kimberly K. Boddy [2]
Matteo Bonato [29]
Julian Borrill [9,10]
François Bouchet [30]
François Boulanger [31]
Blakesley Burkhart [32]
Jens Chluba [33]
David Chuss [11]
Susan E. Clark [18,34]
Joelle Cooperrider [6]
Brendan P. Crill [6]
Gianfranco De Zotti [35]
Jacques Delabrouille [5,12]
Eleonora Di Valentino [36]
Joy Didier [37]
Olivier Doré [6,8]
Hans K. Eriksen [26]
Josquin Errard [5]
Tom Essinger-Hileman [21]
Stephen Feeney [17]
Jeffrey Filippini [38]
Laura Fissel [14]
Raphael Flauger [15]
Unni Fuskeland [26]
Vera Gluscevic [39]
Krzysztof M. Gorski [6]
Dan Green [16]
Shaul Hanany [1]
Brandon Hensley [4]
Diego Herranz [27]
J. Colin Hill [17,18]
Eric Hivon [30]
Renée Hložek [40]
Johannes Hubmayr [19]
Bradley R. Johnson [41]
William Jones [4]
Terry Jones [1]
Lloyd Knox [20]
Al Kogut [21]
Marcos López-Caniego [42]
Charles Lawrence [6]
Alex Lazarian [43]
Zack Li [4]
Mathew Madhavacheril [4]
Jean-Baptiste Melin [12]
Joel Meyers [44]
Calum Murray [5]
Mattia Negrello [45]
Giles Novak [46]
Roger O'Brient [6,8]
Christopher Paine [6]
Tim Pearson [8]
Levon Pogosian [47]
Clem Pryke [1]
Giuseppe Puglisi [48,49]
Mathieu Remazeilles [33]
Graca Rocha [6,8]
Marcel Schmittfull [18]
Douglas Scott [50]
Peter Shirron [21]
Ian Stephens [51]
Brian Sutin [6]
Maurizio Tomasi [52]
Amy Trangsrud [6]
Alexander van Engelen [23]
Flavien Vansyngel [53]
Ingunn K. Wehus [26]
Qi Wen [1]
Siyao Xu [43]
Karl Young [1]
Andrea Zonca [54]

Endorsers

Maximilian Abitbol
Zeeshan Ahmed
David Alonso
Mustafa A. Amin
Adam Anderson
James Annis
Jason Austermann
Carlo Baccigalupi
Darcy Barron
Ritoban Basu Thakur
Elia Battistelli
Daniel Baumann
Karim Benabed
Bradford Benson
Paolo de Bernardis
Marco Bersanelli
Federico Bianchini
Daniel Bilbao-Ahedo
Colin Bischoff
Sebastian Bocquet
J. Richard Bond
Jeff Booth
Sean Bryan
Carlo Burigana
Giovanni Cabass
Robert Caldwell
John Carlstrom
Xingang Chen
Francis-Yan Cyr-Racine
Paolo de Bernardis
Tijmen de Haan
C. Darren Dowell
Cora Dvorkin
Chang Feng
Ivan Soares Ferreira
Aurelien Fraisse
Andrei V. Frolov
Nicholas Galitzki
Silvia Galli
Ken Ganga
Tuhin Ghosh
Sunil Golwala
Riccardo Gualtieri
Jon E. Gudmundsson
Nikhel Gupta
Nils Halverson
Kyle Helson
Sophie Henrot-Versillé
Thiem Hoang
Kevin M. Huffenberger
Kent Irwin
Reijo Keskitalo
Rishi Khatri
Chang-Goo Kim
Theodore Kisner
Arthur Kosowsky
Ely Kovetz
Kerstin Kunze
Guilaine Lagache
Daniel Lenz
François Levrier
Marilena Loverde
Philip Lubin
Juan Macias-Perez
Nazzareno Mandolesi
Enrique Martínez-González
Carlos Martins
Silvia Masi
Tomotake Matsumura
Darragh McCarthy
P. Daniel Meerburg
Alessandro Melchiorri
Marius Millea
Amber Miller
Joseph Mohr
Lorenzo Moncelsi
Pavel Motloch
Tony Mroczkowski
Suvodip Mukherjee
Johanna Nagy
Pavel Naselsky
Federico Nati
Paolo Natoli
Michael Niemack
Elena Orlando
Bruce Partridge
Marco Peloso
Francesco Piacentini
Michel Piat
Elena Pierpaoli
Giampaolo Pisano

Nicolas Ponthieu
Giuseppe Puglisi
Benjamin Racine
Christian Reichardt
Christophe Ringeval
Karwan Rostem
Anirban Roy
Jose Alberto Rubino-Martin
Matarrese Sabino
Maria Salatino
Benjamin Saliwanchik
Neelima Sehgal
Sarah Shandera
Erik Shirokoff
Anže Slosar
Tarun Souradeep
Suzanne Staggs
George Stein
Radek Stompor
Rashid Sunyaev
Aritoki Suzuki
Eric Switzer
Andrea Tartari
Grant Teply
Peter Timbie
Matthieu Tristram
Caterina Umiltà
Rien van de Weygaert
Vincent Vennin
Licia Verde
Patricio Vielva
Abigail Vieregg
Jan Vrtilek
Benjamin Wallisch
Benjamin Wandelt
Gensheng Wang
Scott Watson
Edward J. Wollack
Zhilei Xu
Siavash Yasini

Affiliations

1. University of Minnesota - Twin Cities.
2. Johns Hopkins University.
3. Carnegie Melon University.
4. Princeton University.
5. APC, Univ Paris Diderot, CNRS/IN2P3, CEA/lrfu, Obs de Paris, Sorbonne Paris Cité, France.
6. Jet Propulsion Laboratory, California Institute of Technology.
7. Cornell University.
8. California Institute of Technology.
9. Lawrence Berkeley National Laboratory.
10. Space Sciences Laboratory, University of California, Berkeley.
11. Villanova University.
12. IRFU, CEA, Université Paris-Saclay, France.
13. University of Pennsylvania.
14. National Radio Astronomy Observatory.
15. University of California, San Diego.
16. University of California, Berkeley.
17. Center for Computational Astrophysics, Flatiron Institute.
18. Institute for Advanced Study, Princeton.
19. National Institute of Standards and Technology.
20. University of California, Davis.
21. NASA Goddard Space Flight Center.
22. University of Michigan.
23. Canadian Institute for Theoretical Astrophysics, University of Toronto, Canada.
24. Kavli Institute for the Physics and Mathematics of the Universe (WPI).
25. IRAP, Université de Toulouse, France.
26. University of Oslo, Norway.
27. Instituto de Física de Cantabria (CSIC-Universidad de Cantabria), Spain.
28. School of Physics, Indian Institute of Science Education and Research Thiruvananthapuram, India.
29. INAF-Istituto di Radioastronomia and Italian ALMA Regional Centre, Italy.
30. Institut d'Astrophysique de Paris, CNRS and Sorbonne Université, France.
31. Ecole Normale Superieure, Paris, France.
32. Rutgers University.
33. JBCA, University of Manchester.
34. Hubble Fellow
35. INAF-Osservatorio Astronomico di Padova, Italy.
36. University of Manchester.
37. University of Southern California.
38. University of Illinois, Urbana-Champaign.
39. University of Florida.
40. Department of Astronomy & Astrophysics and Dunlap Institute, University of Toronto, Canada.
41. Columbia University.
42. European Space Astronomy Centre.
43. University of Wisconsin - Madison.
44. Southern Methodist University.
45. Cardiff University School of Physics and Astronomy.
46. Northwestern University.
47. Simon Fraser University.
48. Stanford University.
49. Kavli Institute for Particle Astrophysics and Cosmology.
50. University of British Columbia, Canada.
51. Harvard-Smithsonian Center for Astrophysics.
52. Università degli studi di Milano.
53. Institut d'Astrophysique Spatiale, CNRS, Univ. Paris-Sud, Université Paris-Saclay, France.
54. San Diego Supercomputer Center, University of California, San Diego.

***

This research was funded by a NASA grant NNX17AK52G to the University of Minnesota / Twin Cities, by the Jet Propulsion Laboratory, California Institute of Technology, under a contract with the National Aeronautics and Space Administration, and by Lockheed Martin Corporation.
Substantial contributions to the development of PICO were volunteered by scientists at many institutions world-wide. They are very gratefully acknowledged.

1 Executive Summary

The Probe of Inflation and Cosmic Origins (PICO) is an imaging polarimeter that will scan the sky for 5 years in 21 frequency bands from 21 to 799 GHz. It will produce full-sky surveys of intensity and polarization with a final combined-map noise level equivalent to 3300 *Planck* missions for the baseline required specifications, and according to our current best-estimate would perform as 6400 *Planck* missions. With these capabilities, unmatched by any other existing or proposed platform:

• PICO could determine the energy scale of inflation and give a first, direct probe of quantum gravity by searching for the signal that arises from gravitational waves sourced by inflation and parameterized by the tensor-to-scalar ratio r. The PICO requirement is to detect $r = 5 \times 10^{-4}\,(5\sigma)$, a level that is 100 times lower than current upper limits, and 5 times lower than limits forecast by any planned experiment. If the signal is not detected, PICO is the only instrument that can exclude at 5σ models for which the characteristic scale in the potential is the Planck scale, a key threshold in inflation physics.

• The mission will measure the minimum expected sum of the neutrino masses with 4σ confidence, rising to 7σ if the sum is near 0.1 eV.

• The measurements will either detect or strongly constrain deviations from the standard model of particle physics by counting the number of light particle species $N_{\rm eff}$ in the early universe with $\Delta N_{\rm eff} < 0.06\,(2\sigma)$.

• PICO will elucidate the processes affecting the evolution of cosmic structures by measuring the optical depth to reionization τ with an error $\sigma(\tau) = 0.002$, limited only by the number of spatial modes available in the largest angular scale cosmic microwave background (CMB) polarization.

• The data will give a full sky map of the projected gravitational potential due to all structures in the Universe with the highest signal-to-noise ratio (SNR) relative to any foreseeable experiment, and it will give a catalog of 150,000 clusters extending to their earliest formation redshift. Each of these datasets will be used in combination with other data to constrain the evolution of the amplitude of linear fluctuations $\sigma_8(z)$ with sub-percent accuracy and thus constrain dark energy and modified gravity models.

• PICO will determine the cosmological paradigm of the 2030s by reducing the allowed volume of uncertainty in an 11-dimensional ΛCDM parameter space by a factor of nearly a billion relative to current *Planck* constraints on only six parameters. Such exquisite scrutiny will either give strong validation of the model or require yet-to-be discovered revisions.

• With 86,000,000 independent polarization measurements across the Milky Way, 3,000 times more than *Planck* had, PICO's data will be used to resolve long-standing questions about our Galaxy including the composition, temperature, and emissivities of Galactic dust, and the relative roles of gas turbulence and magnetic fields in the dynamics of the Galaxy and in the observed low star-formation efficiency.

• The data will constrain generic models of dark matter; enable a search for primordial magnetic fields with sufficient sensitivity to rule them out as the sole source for the largest observed galactic magnetic fields; constrain string-theory-motivated axions; and will give precise tracing of the evolution with z of thermal pressure in the universe.

• PICO's deep, full-sky legacy maps will constrain the early phases of galaxy and cluster evolution; perform a census of cold dust in thousands of low z galaxies; make cosmic infrared background maps due to dusty star-forming galaxies; and map magnetic fields in 70 nearby galaxies.

With its broad frequency coverage, PICO is better equipped than any other current or planned instrument to separate the detected signals into their original sources of emission. This capability is important for many of the science goals, and is critical for unveiling the faintest of signals, the telltale signature of inflation, which is already known to be dominated by Galactic foregrounds. PICO's large multiplicity of independent maps and sky surveys, and its stable thermal environment will give control of systematic uncertainties unmatched by any other platform. Mission operations are simple: PICO has a single instrument that surveys the sky with a continuously repetitive pattern. The required technologies have either already been proven by past missions, or are simple extensions of technologies now being used by sub-orbital experiments.

Table 1.1: **Mission Parameters**

Full sky CMB polarization map depth[a] :	
Baseline	0.87 μK_{CMB} arcmin
	equivalent to 3300 *Planck* missions
CBE[b]	0.61 μK_{CMB} arcmin
	equivalent to 6400 *Planck* missions
Survey duration / start .	5 yrs / 2029
Orbit type	Sun-Earth L2
Launch mass	2147 kg
Total power	1320 W
Data rate	6.1 Tbits/day
Cost	$ 958M

[a] rms noise in 1×1 arcmin^2 pixel.
[b] CBE = Current best estimate.

The science PICO will deliver addresses some of the most fundamental quests of human knowledge. Its science advances will enrich many areas of astrophysics, and will form the basis for the cosmological paradigm of the 2030s and beyond. Progress in CMB science requires a scale-up of investment. PICO is the most cost-effective way to achieve this scale-up. It has no competitor in terms of raw sensitivity, and it is the only single-platform instrument with the combination of angular resolution, frequency bands, and control of systematic effects that can deliver the compelling, timely, and broad science.

2 Key Science Goals and Objectives

2.1 Gravitational Waves and Inflation

Measurements of the CMB *BB* angular power spectrum are the only foreseeable way to detect inflationary gravitational waves. The strength of the signal, quantified by the tensor-to-scalar ratio r, is a direct measure of the expansion rate of the Universe during inflation, and together with the Friedmann equation, it reveals the energy scale of inflation. A detection of r "would be a watershed discovery", a quote from the 2010 decadal panel report [1].

PICO will detect primordial gravitational waves at 5σ significance if inflation occurred at an energy scale of at least 5×10^{15} GeV, or equivalently $r = 5 \times 10^{-4}$. In a widely endorsed community white paper setting targets for measurements of inflationary gravitational waves in the next decade, Shandera et al. [2] quote two theoretically motivated r rejection targets: (1) $r < 0.01$, and (2) $r < 0.001$. The second threshold is motivated by the goal of rejecting all inflationary models that naturally explain the observed value of the spectral index n_s and having a characteristic scale in the potential that is larger than the Planck scale. Such models are shown in dashed lines in Figure 2.1. They write "If these thresholds are passed without a detection, most textbook models of inflation will be ruled out; and ... the data would then force a significant change in our understanding of the primordial Universe." PICO is the only next-decade experiment with the raw sensitivity to reject both targets at high confidence; see Figure 2.1. It is the only next-decade experiment that can detect inflationary models that have $r \geq 5 \times 10^{-4}$ at high confidence.

Uncertainty in the characterization of Galactic foregrounds already limits our ability to constrain r. These foregrounds are anticipated to be nearly 1000 times stronger than next-decade-

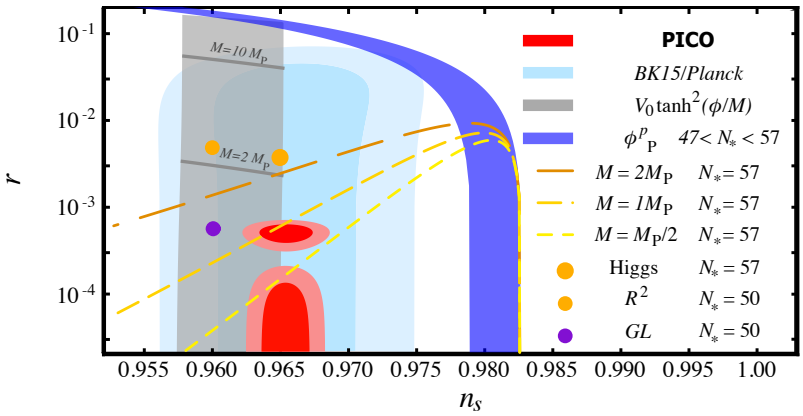

Figure 2.1: PICO will conclusively rule out all Inflation models for which the characteristic scale in the potential is M_p or higher, or will detect $r = 0.0005$ at 5σ (red 1 and 2σ limits and uncertainty ellipses). Current values of σ_r are a factor of 100 higher (cyan). The locus of classes of models and specific ones are shown with dots, solid, and dashed lines.

targeted inflationary B-mode signals at low ℓ multipoles. 'Lensing' B-modes, created by gravitational lensing of E-modes, are an additional effective foreground for the higher multipoles. With sufficiently high resolution to remove at least 73% of the lensing effects, and 21 frequency bands to account for foregrounds, no other next-decade experiment is better equipped than PICO to overcome the challenges in robustly finding the faint inflationary signal, or in rejecting confusion due to foregrounds.

2.2 Fundamental Particles and Fields

• **Light Relics** The effective number of light relic particle species $N_{\rm eff}$ gives information about particle species that are predicted to have existed in the early Universe in extensions of the Standard Model. With three neutrino species $N_{\rm eff} = 3.046$. Additional light particles contribute a change $\Delta N_{\rm eff}$ that is a function only of the decoupling temperature of the additional species and the spin of the particle. PICO will provide a constraint $\Delta N_{\rm eff} < 0.06\,(95\%)$ and will either detect new particle species, or constrain the lowest temperature T_F at which any vector particle (spin 1) could have fallen out of equilibrium to a factor of 400 higher than today's constraint [**?**]. No other next-decade experiment will provide a tighter constraint.

• **Neutrino Mass** The origin, structure, and values of the neutrino masses are among the outstanding questions about the nature of the Standard Model of particle physics. All cosmological measurements of $\sum m_\nu$ relate the amplitudes of the matter power spectrum and the primordial fluctuation power spectrum A_s. Both are limited by degeneracies with other parameters. PICO is the only instrument that will self consistently provide three of the four necessary ingredients [**? ?**]. In combination with ω_m coming from DESI and EUCLID data, PICO will give $\sigma(\sum m_\nu) = 14$ meV, giving a 4σ detection of the minimum sum of 58 meV. PICO will measure $\sum m_\nu$ in two additional ways, which will give equivalent constraints.

• **Dark Matter** CMB experiments are effective in constraining dark matter candidates in the lower mass range, which is not available for terrestrial direct detection experiments [3–8]. PICO's constraining power comes from making high SNR maps of the lensing-induced deflections of polarized photons, and cosmic-variance limited determinations of the TT, TE and EE spectra up to $\ell \simeq 2500$. For a spin-independent velocity-independent contact-interaction between dark matter and protons, chosen as our fiducial model, PICO will improve upon *Planck*'s dark matter cross-section constraints by a factor of 25 over a broad range of candidate dark matter masses. If 2% of the total dark content is made of axions, PICO's measurement of the TT, TE and EE spectra with additional constraints from the lensing reconstruction will detect this species at between 7

and 13σ, depending on the mass range. need to put these constraints in 'next decade' perspective

• **Primordial Magnetic Fields** One of the long-standing puzzles in astrophysics is the origin of observed 1–10 μG galactic magnetic fields [9]. Producing such fields through a dynamo mechanism requires a primordial seed field [10]. Moreover, μG-strength fields have been observed in proto-galaxies that are too young to have gone through the number of revolutions necessary for the dynamo to work [11]. A 0.1 nG primordial magnetic field (PMF), present at the time of galaxy formation, could provide the seed or even eliminate the need for the dynamo altogether [12]. A detection of PMFs with the CMB would be a major discovery because it would signal new physics beyond the Standard Model, and discriminate among different theories of the early Universe [13–15]. PICO will probe PMFs as weak as 0.1 nG (1σ), a precision not attainable by any next-decade experiment, and can thus conclusively rule out the purely primordial (i.e., no-dynamo driven) origin of the largest galactic magnetic fields.

• **Cosmic Birefringence** A number of well-motivated extensions of the Standard Model involve fields with parity-violating coupling [16–18, 18–21]. Their presence may cause cosmic birefringence – a rotation of the polarization of an electromagnetic wave as it propagates across cosmological distances [18, 22, 23]. PICO's constraints on cosmic birefringence are more stringent than any other next-decade experiment [**?**].

2.3 Cosmic Structure Formation and Evolution

• **The Formation of the First Luminous Sources** A few hundred million years after the Big Bang, the neutral hydrogen gas permeating the Universe was reionized by photons emitted by the first luminous sources to have formed. The nature of these sources and the exact history of this epoch are key missing links in our understanding of structure formation. With full sky coverage, multiple frequency bands, and ample sensitivity to remove foregrounds, PICO is uniquely suited to make the low-ℓ EE-spectrum measurements and reach cosmic-variance-limited precision with $\sigma(\tau) = 0.002$, settling some of these questions and significantly constraining the others. Data from PICO's frequency bands above 400 GHz – which have better than 2 arcmin resolution – will be used to provide clean maps for higher resolution ground-based instruments that can reconstruct the patchy τ field. No other experiment can provide these data.

• **Probing the Evolution of Structures via Gravitational Lensing and Cluster Counts** The amplitude of linear fluctuations as a function of redshift, parameterized by $\sigma_8(z)$, is a sensitive probe of physical processes affecting growth of structures in the Universe. CMB photons are affected by, and thus probe, $\sigma_8(z)$ as they traverse the entire Universe. The PICO sub-percent constraints on $\sigma_8(z)$, obtained through measurements of gravitational lensing and independently through using cluster counts, will translate to constraints on dark energy, models of modified gravity, baryonic feedback process, and limits on the particle content of the Universe.

– Gravitational Lensing Matter between us and the last-scattering surface deflects the path of photons through gravitational lensing, imprinting the three-dimensional matter distribution across the volume of the Universe onto the CMB maps. The specific quantity being mapped by these data is the projected gravitational potential ϕ that is lensing the photons. With SNR of more than 560, the PICO $C_L^{\phi\phi}$ angular power spectrum is the highest of any foreseeable CMB experiment in the range $2 \leq L \lesssim 1500$. PICO's ϕ map will be a key ingredient in the delensing process that improves constraints on r, in extracting neutrino mass constraints, in constraining shear biases for LSST and WFIRST [**?**], and in measuring $\sigma_8(z)$ in multiple redshift bins with sub-percent accuracy [24].

– Cluster Counts The distribution of galaxy clusters over redshift is one consequence of the evolution of structures and is thus a sensitive measure of $\sigma_8(z)$. We forecast that PICO will find ∼150,000 galaxy clusters, assuming the cosmological parameters from *Planck* and using the 70% of sky not obscured by the Milky Way. Information provided by the high frequency bands will mitigate the potential reduction in detection efficiency due to dust emission by cluster members [25]. This catalog will provide σ_8 with sub-percent precision for $0.5 < z < 2$, and a neutrino mass constraint $\sigma(\sum m_\nu) = 14$ meV that is independent from the one coming from the CMB lensing measurements. A significant fraction of the PICO-detected clusters will also be detected by eROSITA, giving an exceptional catalog of multi-wavelength observations for detailed studies of cluster astrophysics.

• **Constraining Feedback Processes through the Sunyaev–Zeldovich Effect** About 6% of CMB photons are Thomson-scattered by free electrons in the intergalactic medium (IGM) and intercluster medium (ICM), and a fraction of these are responsible for the thermal and kinetic Sunyaev–Zeldovich effects (tSZ and kSZ) [26, 27]. The amplitude of the tSZ is proportional to the integrated electron pressure along the line of sight, and it thus contains information about the thermodynamic properties of the IGM and ICM, which are highly sensitive to astrophysical feedback. With its low noise and broad frequency coverage, which is essential for separating out other signals, PICO will yield a definitive tSZ map over the full sky with a total SNR of 1270 for the CBE and 10% lower for the baseline configurations (Fig. **??**). what is unique? Full sky? frequencies? resolution? The 150,000 clusters forecast to be detected by PICO will be found in this map. Considering the LSST gold weak-lensing sample, with a source density of 26 galaxies/arcmin^2 covering 40% of the sky, we forecast a detection of the tSZ–weak-lensing cross-correlation with SNR = 3000. Cross-correlations with the galaxies themselves will be measured at even higher SNR. At this immense significance, the signal will be broken down into dozens of tomographic redshift bins, precisely tracing the evolution of thermal pressure over cosmic time.

2.4 Testing ΛCDM

PICO will set the cosmological paradigm for the 2030's and beyond by measuring the six parameter ΛCDM with 100,000 more constraining power compared to *Planck*; see Figure 2.4 (the improvement between WMAP and Planck was by 100). For an 11-parameter set that include r, $N_{\rm eff}$, and $\Sigma(m_\nu)$, the improvement is by a factor of 0.5×10^9. These improvements will test ΛCDM so stringently that it is hard to imagine it surviving such a scrutiny if it is not fundamentally correct. If tensions deepen to become discrepancies, it would be even more exciting if a new cosmological model emerged.

2.5 Galactic Structure and Star Formation

PICO will produce 21 polarization maps of Galactic emission, all much deeper than *Planck*'s seven maps. At 799 GHz PICO will have five times finer resolution than *Planck*; see Fig. **??**). Such a data set can only be obtained by PICO. These data will complement a rich array of other polarization observations forthcoming in the next decade, including stellar polarization surveys to be combined with Gaia astrometry, and Faraday rotation measurements from observations at radio wavelengths with the Square Kilometer Array (SKA) and its precursors.

• **Test models of the composition of interstellar dust** Less than 1 μm in size, dust grains are intermediate in the evolution from atoms and molecules to large solid bodies such as comets,

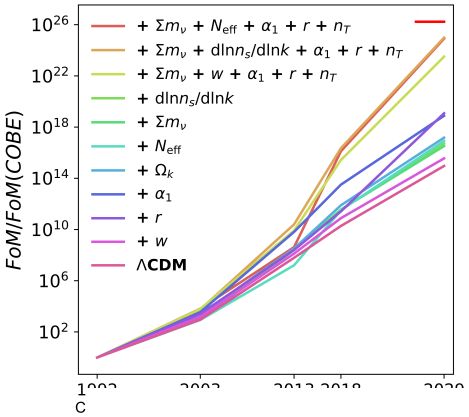

Figure 2.2: The increase in cosmological parameter constraining power using only CMB data since *COBE*. The FoM is the inverse of the uncertainly volume in parameter space. For an 11-parameter set that includes $N_{\rm eff}$ (red increasing line) PICO will improve the FoM by a factor of 0.5×10^9 relative to *Planck*. It will extract nearly the same information as that attainable by a mission with twice higher resolution and nine times lower noise (top right red horizontal bar), that is, PICO's performance on cosmological parameters is equivalent to that of a 'CMB flagship-scale mission'. The constituents of the 11-parameter set are given in Hanany et al. [24].

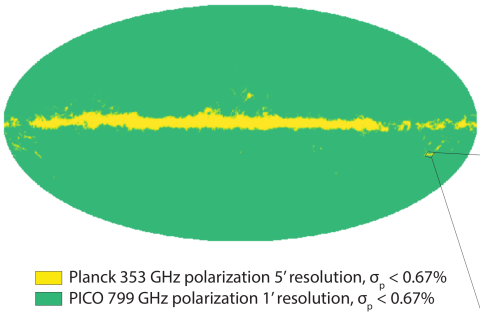

Figure 2.3: Caption will be here

asteroids, and planets. Through vastly improved spectral characterization of Galactic polarization, the PICO data will validate or reject state-of-the-art dust models [e.g. 28, 29], test for the presence of additional dust grain species with distinct polarization signatures, such as magnetic nanoparticles [30], and will be used as an input for the foreground separation necessary to extract cosmological *E*- and *B*-mode science.

• **Determine how magnetic fields affect molecular cloud and star formation** Stars are formed through interactions between gravitational and magnetic fields, turbulence, and gas over more than four orders of magnitude of spatial scales, which span the diffuse ISM (kpc scale), molecular clouds (10 pc), and molecular cloud cores (0.1 pc). However, the role magnetic fields play in the large-scale structure of the diffuse interstellar medium (ISM) and in the observed low star-formation efficiency has been elusive, owing to the dearth of data. With $1.1'$ resolution PICO will expand the number of independent magnetic field measurements across the sky by a factor of 2900, from *Planck*'s 30,000 to 86,000,000 (Fig. **??**). The data will robustly characterize turbulent properties like the Alfvén Mach number across a previously unexplored regime of parameter space.

2.6 Legacy Surveys

PICO will generate a rich and unique catalog of hundreds of thousands of new sources serving astrophysicists across a broad range of interests including in galaxy and cluster evolution, correlations of cold galactic dust with galaxy properties, the physics of jets in active galactic nuclei, and the properties of the cosmic infrared background. This information will be embedded in catalogs including 50,000 proto-clusters extending to $z \simeq 4.5$, 4,500 strongly lensed galaxies extending to $z \simeq 5$, 30,000 galaxies with $z \leq 0.1$, polarization data for few thousand radio sources and dust galaxies, and the deepest maps of the CIB with as high a resolution as $1'$.

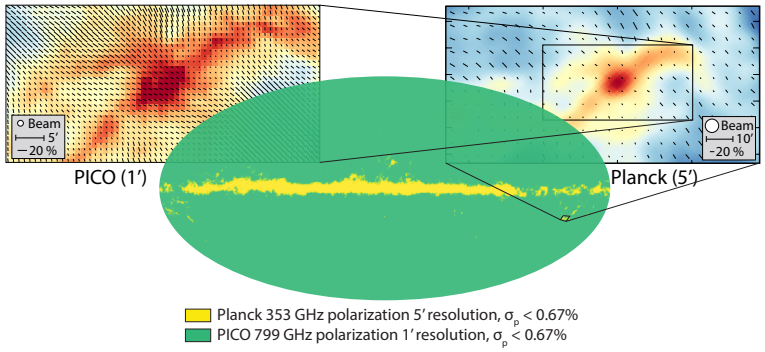

Figure 2.4: Caption will be here

2.7 Signal Separation

2.7.1 The Signal Separation Challenge

Galactic emission dominates the sky's polarized intensity on large angular scales ($\ell \lesssim 10$), it dominates the cosmological B-modes signals for $\ell \lesssim 150$ for all allowed levels of r, and it is expected to be significant even at $\ell \simeq 1000$, posing challenge for reconstructing the B-mode signal from lensing. This is illustrated in Figs. **??** and 2.5, which show Galactic emission power spectra calculated for the cleanest – that is, the least Galactic-emission-contaminated – 60% of the sky. But even in small patches of the sky, far from the Galactic plane and with the least foreground contamination, Galactic emission levels are substantial relative to an inflationary signal of $r \sim 0.01$ [31]. Separating the cosmological and Galactic emission signals is one of two primary challenges facing any next-decade experiment attempting to reach these levels of constraints on r (the second is control of systematic uncertainties).

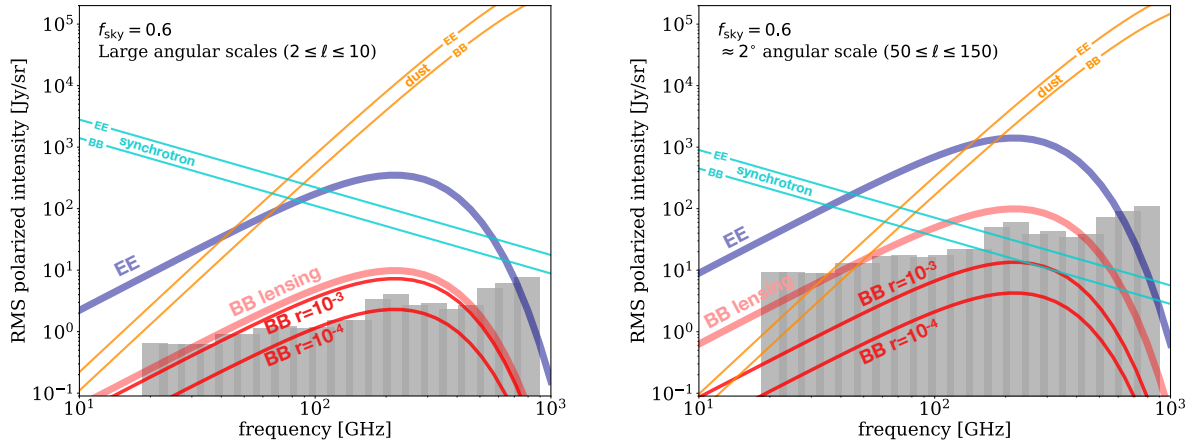

Figure 2.5: Polarization BB spectra of Galactic synchrotron and dust, compared to CMB polarization EE and BB spectra of different origins for two values of r and for two ranges of angular scales: large-scale, $\ell \leq 10$, corresponding to the reionization peak (left panel); and intermediate scales $50 \leq \ell \leq 150$, corresponding to the recombination peak (right panel). Data from *Planck* indicate that for Galactic emission the level of the E-mode is approximately twice that of B [31]. The PICO baseline noise (grey bands) is low compared to the Galactic emission components, and thus they will be measured with high SNR in many frequency bands.

To investigate the efficacy of PICO in addressing the foreground-separation challenge, we used both an analytic forecast and map-domain simulations; a complete description is given in Hanany et al. [24]. Here we present results only from the more conservative map-domain analysis. In this analysis we simulate sky maps that are constrained by available data, but otherwise have a mixture

of foreground properties; we 'observe' these maps just like a realistic experiment would do, and then apply foreground separation techniques to separate the Galactic and CMB emissions. Our results indicate that:

• the combination of PICO's sensitivity and broad frequency coverage are effective in foreground removal and that PICO will reach the requirement of $r = 5 \times 10^{-4}\,(5\sigma)$; see Figure 2.6; • the high frequency bands, above 400 GHz, may be essential for proper subtraction of foregrounds; see Figure 2.7.

Among all next decade experiments, PICO is best suited to handle and model the foregrounds because it has more frequency bands than any other experiment, because it has the lowest noise, and because it has full sky coverage, giving access to several independent small regions that are very low in dust emission. This is a distinct advantage relative to CMB-S4, which targets a single patch of the sky, and relative to liteBIRD, which does not have frequency bands above 400 GHz.

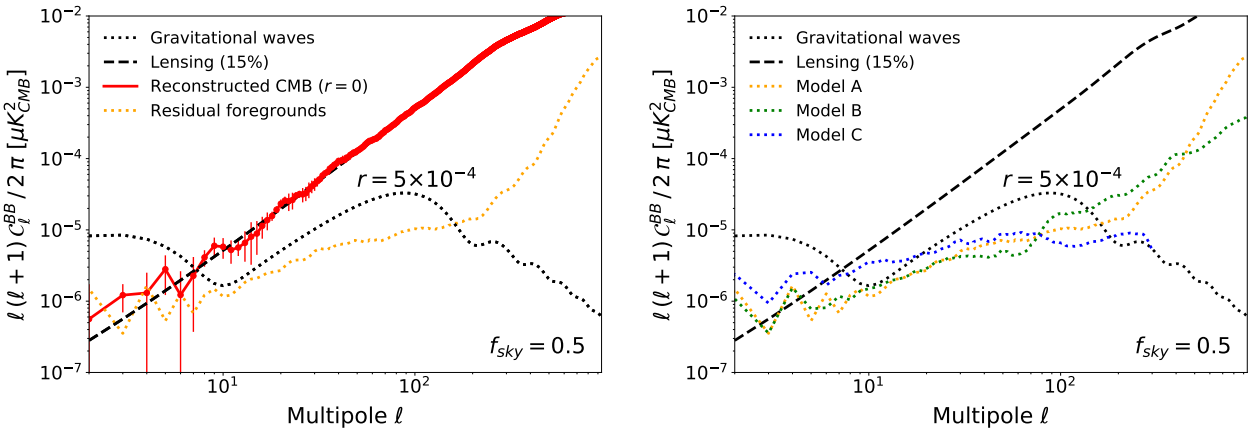

Figure 2.6: Angular power spectra of *BB* due to the CMB and of residual foregrounds after an end-to-end map-based foreground-separation exercise. The PICO low noise levels and breadth in frequency coverage enable separation of model A foregrounds such that the residual foreground spectrum (left, yellow dotted) is a factor of ten (four) below a *BB* inflationary signal with $r = 5 \times 10^{-4}$ (black dotted) at $\ell = 5(80)$. Within errors, the recovered CMB (red) matches the input CMB, which consists of only lensing *BB* (dashed black), over all angular scales $\ell \gtrsim 6$. The results for model B are similar (right, green dots), while model C has somewhat higher residuals at low ℓ. In this exercise we used 50% of the sky. Lower foreground residual levels are obtainable with smaller, cleaner patches of ∼5% of sky, which would reduce the residual foregrounds at $\ell \simeq 80$.

2.8 Systematic Uncertainties

Properly modeling, engineering for, and controlling systematic effects are key for the success of any experimental endeavor striving to achieve $\sigma(r) \lesssim 1 \times 10^{-3}$. Based on extensive community experience with both hardware and analysis of data we make the following points.

- Relative to other platforms, a space-based mission provides the most thermally stable platform, and thus the prerequisite for improved control of systematic effects. PICO's orbit at L2 is among the most thermally stable of possible orbits.
- PICO's sky scan pattern gives strong data redundancy, which enables numerous cross-checks. Each of the 12,996 detectors makes independent maps of the I, Q, and U Stokes parameters enabling many comparisons within and across frequency bands, within and across sections of the focal plane, and within and across bolometers that have either the same or different polarization sensitivities. Half the sky is scanned every two weeks, and the entire sky is scanned in 6 months.

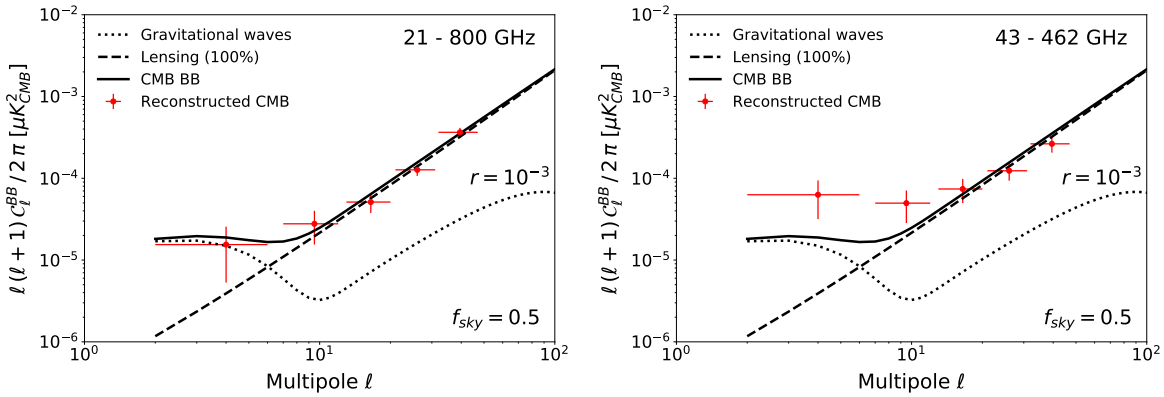

Figure 2.7: **Left:** Foreground separation with all of PICO's 21 frequency bands recovers the input CMB *BB* power spectrum (solid black) without bias (red). The input CMB spectrum has a contribution from lensing (dashed) and an inflationary signal with $r = 0.001$ (dotted). This exercise uses a parametric approach [32] with foregrounds varying on 4° pixels, and using 50% sky fraction. **Right:** Running the same foreground separation algorithm on the same sky but using only PICO's bands between 43 and 462 GHz produces an output spectrum (red) that is biased at low multipoles relative to the input. With real data, such a bias would be erroneously interpreted as a higher value of r.

Thus combinations of maps constructed at different times during of the mission will be differenced to search for residual time-dependent systematic effects.

- The scan pattern gives almost continuous scans of planets and large amplitude (≥ 4 mK) CMB dipole signals [33]. These features result in continuous, high SNR calibration and antenna-pattern characterization. In comparison, *Planck* observed each of the planets with only a 6 month cadence and had nearly 100 days/year during which the dipole calibration signals were below 4 mK, at times dipping below 1 mK.
- We showed that two of the highest priority systematic effects can be controlled to levels that are small compared to requirements. More analysis and planning is required to address systematic uncertainties arising from the far-sidelobe response of the telescope.

We direct the reader to the mission study report for more details on our work on systematic effects for PICO [24].

3 Technical Overview

PICO meets all of its science-driven instrument requirements with a single instrument: an imaging polarimeter with 21 logarithmically spaced frequency bands centered between 21 and 799 GHz (Table **??**). The instrument has a two-reflector Dragone-style telescope; see Figure. 3.1. The focal plane is populated by transition-edge-sensor (TES) bolometers and read out using a time-domain multiplexing scheme. The instrument has both passive and active cooling stages. PICO operates from the Earth-Sun L2 and employs a single science observing mode, providing highly redundant coverage of the full sky. A full description of the reference design is given by Hanany et al. [24].

3.1 Telescope, Detectors, and Readout

The PICO telescope gives a large diffraction-limited field of view, sufficient to support approximately 10^4 detectors; arcminute resolution at 800 GHz; low instrumental and cross-polarization; and low sidelobe response. All requirements are met with PICO's 1.4 m aperture modified open-Dragone design. There are no moving parts in the PICO optical system. There are no lenses, eliminating absorption and reflection losses and obviating the need for anti-reflection coatings.

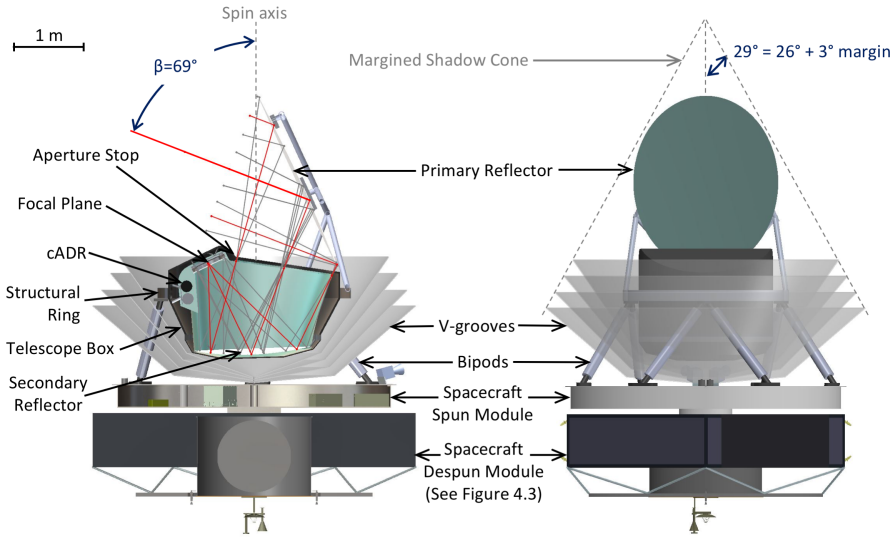

Figure 3.1: PICO overall configuration in side view and cross section (left), and front view with V-Groove assembly shown semi-transparent (right). The mission consists of a single science instrument mounted on a structural ring. The ring is supported by bipods on a stage spinning at 1 RPM relative to a despun module. Only power and digital information pass between the spun and despun stages.

The primary mirror is passively cooled to ∼20 K. An aperture stop and a secondary mirror are actively cooled to 4.5 K.

The sensitivity of PICO's detectors is limited by irreducible backgrounds: the CMB at frequencies below 400 GHz, and emission from the cold primary mirror at higher frequencies. Therefore, the required sensitivity determines the detector count in each band. The PICO focal plane has 12,996 detectors, 175 times the number flown aboard *Planck*, thereby providing the required increase in raw sensitivity. To achieve similar raw sensitivity to PICO, a ground-based instrument would require ∼50 times the number of detectors, and therefore a massive array of cryogenic receivers.

The PICO baseline focal plane employs three-color sinuous antenna/lenslet pixels [*34*] for the 21–462 GHz bands. Niobium microstrips mediate the signals between the antenna and detectors, and partition the wide continuous bandwidth into three narrow channels using integrated, on-wafer, micro-machined filter circuits [*35*]. Six transition edge sensor bolometers per pixel detect the radiation in two orthogonal polarization states.

PICO's highest three frequency channels are beyond the niobium superconducting band-gap, rendering on-wafer, microstrip filters a poor solution for defining the optical passband. For these bands we use feedhorns to couple the radiation to two single-color polarization-sensitive TES bolometers. The waveguide cut-off defines the lower edge of the band, and quasi-optical metal-mesh filters define the upper edge. Numerous experiments have successfully used similar approaches [*36*–*38*].

Polarimetry is achieved by measuring the signals from pairs of two co-pointed bolometers within a pixel that are sensitive to two orthogonal linear polarization states. Half the pixels in the focal plane are sensitive to the Q and half to the U Stokes parameters of the incident radiation, providing sensitivity to the Stokes I, Q, and U parameters. Two layouts for the distribution of the Q and U pixels on the focal plane have been investigated [*39*]; both satisfy mission requirements.

The current baseline for PICO is to use a time-domain multiplexer (TDM), because to date this scheme uses the least power consumption and dissipation at ambient temperatures. The thermal loading on the cold stages from the wire harnesses is subdominant to conductive loading through the mechanical support structures. In the PICO TDM implementation a row of 102 detectors are

readout simultaneously, and 128 such rows are readout sequentially. SQUIDs will be used as current amplifiers. Suborbital experiments have developed techniques to shield the SQUIDs from Earth's magnetic field [40]. Total suppression factors better than 10^7 have been demonstrated [41]. PICO will use these demonstrated techniques to shield SQUID readout chips from the ambient magnetic environment, which is 20,000 times smaller than near Earth.

3.2 Thermal

The PICO thermal system does not require cryogenic consumables, permitting consideration of significant mission extension beyond the prime mission. The system, consisting of V-groove radiators for passive cooling, mechanical coolers to achieve 4.5 K, and a continuous adiabatic demagnetization refrigerator (cADR), meets all thermal requirements with robust margins [24] .

A multi-stage continuous adiabatic demagnetization refrigerator (cADR) maintains the PICO focal plane at 0.1 K and the surrounding enclosure, filter, and readout components at 1 K. Heat loads in the range of 30 μW at 0.1 K and 1 mW at 1 K (time-average) are within the capabilities of current cADRs developed by GSFC [42, 43] and flown on suborbital balloon flights. The PICO sub-kelvin heat loads are estimated at less than half of this capability.

A cryocooler system similar to that used on JWST to cool the MIRI detectors [44, 45] backs the cADR and cools the aperture stop and secondary reflector to 4.5 K. Both Northrop Grumman Aerospace Systems (NGAS, which provided the MIRI coolers) and Ball Aerospace have developed such coolers under the NASA-sponsored Advanced Cryocooler Technology Development Program [46]. The NGAS project has completed PDR-level development, and is expected to reach CDR well before PICO begins Phase-A. The projected performance of this cooler will give more than 100 % heat lift margin relative to PICO's requirements [24].

3.3 Instrument Integration and Test

The PICO instrument integration and testing plan benefits from heritage and experience with the *Planck* HFI instrument [47]. Detector wafers are screened prior to selection of flight wafers and focal-plane integration. The cADR and 4 K cryocooler vendors will qualify those subsystems prior to delivery. The relative alignment of the two reflectors is determined under in-flight thermal conditions using a thermal vacuum (TVAC) chamber and photogrammetry. The flight focal-plane assembly and flight cADR are integrated and tested in a dedicated sub-kelvin cryogenic testbed. The noise, responsivity, and focal-plane temperature stability are characterized using a representative optical load for each frequency band (temperature-controlled blackbody). The same testbed is used to perform the polarimetric and spectroscopic calibration.

The focal plane is integrated with the reflectors and structures, and alignment verified with photogrammetry at cold temperatures in a TVAC chamber. The completely integrated observatory (instrument and spacecraft bus) is tested in TVAC to measure parasitic optical loading from the instrument, noise, microphonics, and RFI. The observatory is 4.5 m in diameter and 6.1 m tall. There are no deployables.

3.4 Design Reference Mission

The PICO concept of operations is similar to that of the successful *WMAP* [48] and *Planck* [49] missions. After launch, PICO cruises to a quasi-halo orbit around the Earth–Sun L2 Lagrange point. A two-week decontamination period is followed by instrument cooldown, lasting about two months. After in-orbit checkout is complete, PICO begins its science survey. During the

survey the instrument spins around the spacecraft's symmetry axis at 1 RPM. The symmetry axis precesses around the anti-sun direction with a period of 10 hours; See Figure 3.3. This survey ensures that each sky pixel is revisited along many orientations, which is optimal for polarimetric measurements. Nearly 50% of the sky are surveyed every two weeks. The entire sky is covered in 6 months. Over the 5 year duration, PICO executes 10 independent full sky surveys, giving high redundancy for identifying systematic uncertainties.

Instrument data are compressed and stored on-board, then returned to Earth in daily 4-hr Ka-band science downlink passes (concurrent with science observations). High data-rate downlink to the Deep Space Network (DSN) is available from L2 using near-Earth Ka bands. We assumed a launch with the Falcon 9. Its capability for ocean recovery exceeds PICO's 2147 kg total launch mass (including contingency) by a 50 % margin.

The PICO spacecraft bus is Class B and designed for a minimum lifetime of 5 years in the L2 environment. Mission-critical elements are redundant. The aft end of the spacecraft (the "de-spun module") is comprised of six equipment bays that house standard components. The instrument and V-grooves are mounted on bipods from the spacecraft's "spun module," which contains the 4 K cooler compressor and drive electronics, the sub-K cooler drive electronics, and the detector warm readout electronics. A motor drives the spun module at 1 rpm. Only power and data (digital) lines pass between the spun and de-spun modules. Reaction wheels on the despun module cancel the angular momentum of the spun module and provide three-axis control.

3.5 Technology Drivers

PICO builds off of the heritage of *Planck*-HFI and *Herschel*. Since the time of *Planck* and *Herschel*, suborbital experiments have used monolithically fabricated TES bolometers and multiplexing schemes to field instruments with thousands of TES bolometers per camera (Fig. **??**).

The remaining technology developments required to enable the PICO baseline design are:

1. extension of three-color antenna-coupled bolometers down to 21 GHz and up to 462 GHz (§ **??**);
2. construction of high-frequency direct absorbing arrays and laboratory testing (§ **??**);
3. beam line and 100 mK testing to simulate the cosmic ray environment at L2 (§ **??**);

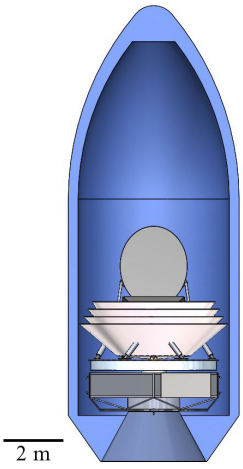

Figure 3.2: PICO is compatible with the Falcon 9.

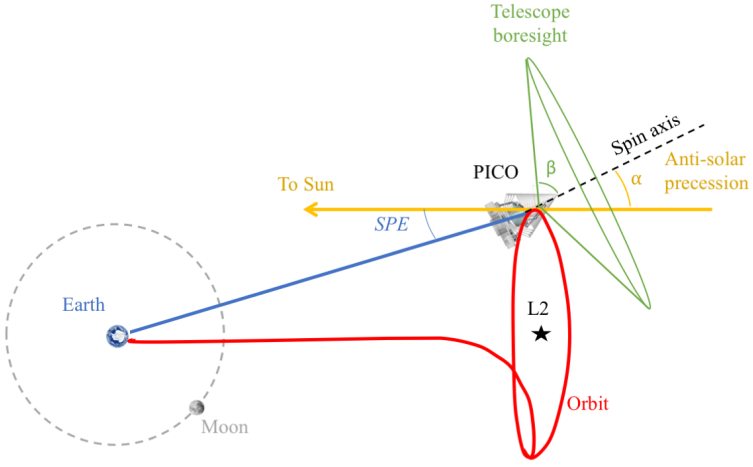

Figure 3.3: PICO surveys by continuously spinning the instrument about a precessing axis.

Table 3.1: PICO technologies can be developed to TRL 5 prior to a 2023 Phase A start using the APRA and SAT programs, requiring a total of about $ 13M. Per NASA guidance, these costs are outside the mission cost (§ **??**).

Task	Current status	Milestone A	Milestone B	Milestone C	Current funding	Required funding	Date TRL5 achieved
1a. Three-color arrays $\nu < 90$ GHz	2-color lab demos $\nu > 30$ GHz	Field demo of 30–40 GHz (2020)	Lab demos 20–90 GHz (2022)	—	APRA & SAT	$2.5M over 4 yr (1 APRA + 1 SAT)	2022
1b. Three-color arrays $\nu > 220$ GHz	2-color lab demos $\nu <$ 300 GHz	Field demo of 150–270 GHz (2021)	Lab demos 150-460 GHz (2022)	—	APRA & SAT	$3.5M over 4 yr (2 SATs)	2022
2. Direct absorbing arrays $\nu > 50$ GHz	0.1–5 THz unpolarized	Design & prototype of arrays (2021)	Lab demo of 555 GHz (2022)	Lab demo of 799 GHz (2023)	None	$2M over 5 yr (1 SAT)	2023
3. Cosmic ray studies	250 mK w/ sources	100 mK tests with sources (2021)	Beamline tests (2023)	—	APRA & SAT	$0.5–1M over 5 yr (part of 1 SAT)	—
4a. Fast readout electronics	MUX66 demo	Engineering and Fab of electronics (2020)	Lab demo (2021)	Field demo (2023)	No direct funds	$4M over 5 yr (1 SAT)	2023
4b. System engineering; 128× MUX demo	MUX66 demo	Design of cables (2020)	Lab demo (2021)	Field demo (2023)	No direct funds	—	—

Table 3.2: Multiple active suborbital efforts are advancing technologies relevant to PICO.

Project	Type	Optical Coupling	ν_c [GHz]	Colors per pixel	$N_{\rm bolo}$	Significance	Reference
PICO baseline	Flight		21 – 462	Three	11,796		§ **??**
SPT-3G	Ground	Sinuous	90 – 220	Three	16,260	Trichroic	[*50*]
Advanced ACT-pol .	Ground	Horns	27 – 230	Two	3,072	Dichroic	[*51*]
BICEP/Keck	Ground	Antenna arrays	90 – 270	One	5,120	50 nK-deg	[*52*]
Berkeley, Caltech, NIST	Lab	Various	30 – 270	Various	–	Band coverage	[*40*, *53*, *54*]
SPIDER	Balloon	Antenna arrays	90 – 285	One	2,400	Stable to 10 mHz	[*55*]

4. expansion of time-division multiplexing to support 128 switched rows per readout column (§ **??**).

All of these developments are straightforward extensions of technologies already available today, with heritage on suborbital missions (See Table **??**. We recommend continued support to complete development of these technologies through the milestones described in Table 3.1. A detailed discussion of these technical challenges is included in the full PICO report [*24*]

Table 3.3: PICO high-frequency detectors leverage development and demonstration by *Planck*, *Herschel*, and SPT.

Project	Type	Polarized	Mono-lithic	ν_c [GHz]	Colors per pixel	$N_{\rm bolo}$	Significance	Reference
PICO baseline	Flight	Yes	Yes	555 – 799	One	1,200		§ **??**
Planck HFI	Flight	143–343 GHz	No	143 – 857	One	48	TRL 9 polarized	[38]
Herschel	Flight	No	Yes	570 – 1200	One	270	TRL 9 monolothic	[56]
SPT-SZ	Ground	No	Yes	90 – 220	One	840	Monolithic array TESs	[36]
SPT-pol-90	Ground	Yes	No	90	One	180	Dual pol absorbing TESs	[57]

4 Organization, Partnerships, and Current Status

PICO is the result of an 18-months mission study funded by NASA (total grant = $150,000). The study was open to the entire mm/sub-mm community. Seven working groups were led by members of PICO's Executive Committee, which had a telephone conference weekly, led by the PI. A three-member steering committee, composed of two experimentalists experienced with CMB space missions, and a senior theorist gave occasional advice to the PI. More than 60 scientists, international- and US-based, participated in-person in each of two community workshops (November 2017 and May 2018). The study report has been submitted by NASA to the decadal panel, and it is available on the arXiv and on the PICO website [24, 58]. It has contributions from 82 authors, and has been endorsed by additional 131 members of the community.

The PICO team designed an entirely US-based mission, so that the full cost of the mission can be assessed. We excluded contributions by other space agencies, despite expression of interest by international scientists. The PICO concept has wide support in the international community. If the mission is selected to proceed, a path that would be scientifically and financially optimal relative to other options, it is reasonable to expect that international partners would participate and thus reduce the US cost of the mission.

5 Schedule and Cost

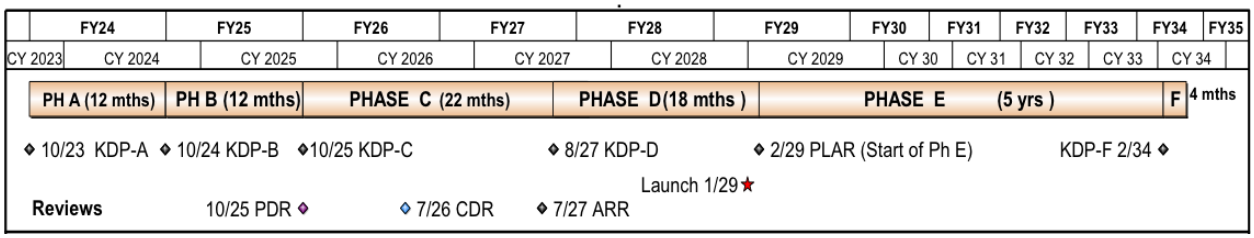

Figure 5.1: PICO development and operations schedule.

• **Schedule** NASA-funded Probe studies including PICO assume a Phase A start in October 2023. PICO development phases B-D are similar in duration to recent comparably sized NASA missions such as Juno and SMAP. PICO is a cryogenic mission similar to *Planck*, but the cryogenic design is simpler because all PICO's bolometric detectors are maintained at 0.1 K

Table 5.1: Detailed breakdown of Team X and PICO Team cost estimates (in FY18$). Costs are based on the schedule in Fig. 5.1, which includes 5 years of operations.

Work Breakdown Structure (WBS) elements	Team X	PICO
Development Cost (Phases A–D)	$ 724M	$ 634–677M
1.0, 2.0, 3.0 Management, Systems Engineering, and Mission Assurance	$ 54M	$ 47– 50M
4.0 Science		$ 19M
5.0 Payload System		$ 168M
6.0 Flight System	$ 248M	$ 210–240M
10.0 Assembly, Test, and	$ 24M	

(*Planck*'s bolometers were maintained at 0.1 K, and the radiometers at 20 K). We used experience from *Planck* and from current implementations of ground-based kilo-pixel arrays to allocate appropriate time for integration and testing (I&T).

The baseline mission lifetime is 5 years. The PICO instrument does not have cryogenic consumables (as Planck did), permitting mission extension beyond the prime mission duration.

• **Cost** We estimate PICO's total Phase A–E lifecycle cost between $870M and $960M, including the $150M allocation for the Launch Vehicle (per NASA direction). These cost estimates include 30 % reserves for development (Phases A–D) and 13 % reserves for operations (Phase E). Table 5.1 shows the JPL Team X and the PICO team mission cost breakdown. Team X estimates are generally model-based, and were generated after a series of instrument and mission-level studies. The PICO team adopted the Team X estimates, but also obtained a parametrically estimated cost range for the Flight System and Assembly, Test, and Launch Operations from Lockheed Martin Corporation to represent the cost benefits that might be realized by working with an industry partner. After adding estimated JPL overhead the PICO team cost is in-family with but lower than the Team X cost.

Science team costs are assessed by Team X based on PICO science team estimates of the numbers and types of contributors and meetings required for each year of PICO mission development and operations. These workforce estimates are informed by recent experience with the *Planck* mission. PICO's spacecraft cost reflects a robust Class B architecture. Mission-critical elements are redundant. Appropriate flight spares, engineering models and prototypes are included. Mission operations, Ground Data Systems, and Mission Navigation and Design costs reflect the relatively simple operations: PICO has a single instrument and a single, repetitive science observing mode.

The active cooling system (the 0.1 K cADR and 4 K cryocooler) comprises nearly half of the payload cost. The cADR cost for this study is an estimate from Goddard Space Flight Center. The 4 K cryocooler cost for this study is based on the NASA Instrument Cost Model (NICM) VIII CER Cryocooler model [*59*], assuming a commercial build. Based on JPL experience, 18 % of the instrument cost is allocated for integration and testing (I&T). More details on the cost of PICO are available in the full PICO report [*24*].

5.1 Heritage

PICO's reflectors are similar to *Planck*'s, but somewhat larger (270 cm × 205 cm primary versus 189 cm × 155 cm) [*60*]. *Herschel* observed at shorter wavelengths that required higher surface accuracy and had a larger reflector (350 cm diameter primary) [*61*]. PICO's detectors are cooled by a cADR with requirements that are within the capabilities of current ADRs developed by Goddard Space Flight Center. These systems have been applied to several JAXA missions, including *Hitomi* [*43*]. PICO's 4 K cryocooler (§ **??**) is a direct extension of the JWST MIRI design [*44*, *45*].

PICO benefits from a simpler and more reliable implementation of the J-T system than was required for MIRI, in that no deployment of cooling lines is required, and all flow valving is performed on the warm spacecraft. Structures similar to PICO's V-groove radiator assembly are a standard approach for passive cooling, and were first described more than thirty years ago [*62*]. PICO's spin system is less demanding than the successful SMAP spin system. The PICO spin rate is 1 rpm, and the mission requires $\sim 220\,\mathrm{N\,m\,s}$ of spin angular momentum cancellation. The PICO's data volume and downlink rates are already surpassed by missions in development.

References

[1] National Research Council, *New Worlds, New Horizons in Astronomy and Astrophysics*. Washington, DC: The National Academies Press, 2010. https://www.nap.edu/catalog/12951/new-worlds-new-horizons-in-astronomy-and-astrophysics

[2] S. Shandera, P. Adshead, M. Amin *et al.*, "Probing the origin of our Universe through cosmic microwave background constraints on gravitational waves," in *Bulletin of the American Astronomical Society*, ser. *Bull. Am. Astron. Soc.*, vol. 51, May 2019, p. 338. https://ui.adsabs.harvard.edu/abs/2019BAAS...51c.338S

[3] T. R. Slatyer, N. Padmanabhan, and D. P. Finkbeiner, "Cmb constraints on wimp annihilation: Energy absorption during the recombination epoch," *Physical Review D (Particles, Fields, Gravitation, and Cosmology)*, vol. 80, no. 4, p. 043526, 2009. http://link.aps.org/abstract/PRD/v80/e043526

[4] S. Galli, F. Iocco, G. Bertone, and A. Melchiorri, "CMB constraints on dark matter models with large annihilation cross section," *Phys. Rev. D.*, vol. 80, no. 2, pp. 023 505–+, Jul. 2009. http://adsabs.harvard.edu/abs/2009PhRvD..80b3505G

[5] G. Hütsi, A. Hektor, and M. Raidal, "Constraints on leptonically annihilating dark matter from reionization and extragalactic gamma background," *Astron. Astrophys.*, vol. 505, pp. 999–1005, Oct. 2009. http://adsabs.harvard.edu/abs/2009A%26A...505..999H

[6] G. Hütsi, J. Chluba, A. Hektor, and M. Raidal, "WMAP7 and future CMB constraints on annihilating dark matter: implications for GeV-scale WIMPs," *Astron. Astrophys.*, vol. 535, p. A26, Nov. 2011. http://adsabs.harvard.edu/abs/2011A%26A...535A..26H

[7] M. S. Madhavacheril, N. Sehgal, and T. R. Slatyer, "Current dark matter annihilation constraints from CMB and low-redshift data," *Phys. Rev. D.*, vol. 89, no. 10, p. 103508, May 2014. http://adsabs.harvard.edu/abs/2014PhRvD..89j3508M

[8] D. Green, P. D. Meerburg, and J. Meyers, "Aspects of Dark Matter Annihilation in Cosmology," *ArXiv e-prints*, Apr. 2018. http://adsabs.harvard.edu/abs/2018arXiv180401055G

[9] L. M. Widrow, "Origin of galactic and extragalactic magnetic fields," *Reviews of Modern Physics*, vol. 74, pp. 775–823, 2002. http://adsabs.harvard.edu/abs/2002RvMP...74..775W

[10] L. M. Widrow, D. Ryu, D. R. G. Schleicher, K. Subramanian, C. G. Tsagas, and R. A. Treumann, "The First Magnetic Fields," *Space Science Reviews*, vol. 166, pp. 37–70, May 2012. http://adsabs.harvard.edu/abs/2012SSRv..166...37W

[11] R. M. Athreya, V. K. Kapahi, P. J. McCarthy, and W. van Breugel, "Large rotation measures in radio galaxies at Z > 2," *Astron. Astrophys.*, vol. 329, pp. 809–820, Jan. 1998. http://adsabs.harvard.edu/abs/1998A%26A...329..809A

[12] D. Grasso and H. R. Rubinstein, "Magnetic fields in the early Universe," *Physics Reports*, vol. 348, pp. 163–266, Jul. 2001. http://adsabs.harvard.edu/abs/2001PhR...348..163G

[13] N. Barnaby, R. Namba, and M. Peloso, "Observable non-Gaussianity from gauge field production in slow roll inflation, and a challenging connection with magnetogenesis," *Phys. Rev. D.*, vol. 85, no. 12, p. 123523, Jun. 2012. http://adsabs.harvard.edu/abs/2012PhRvD..85l3523B

[14] A. J. Long, E. Sabancilar, and T. Vachaspati, "Leptogenesis and primordial magnetic fields," *JCAP*, vol. 2, p. 036, Feb. 2014. http://adsabs.harvard.edu/abs/2014JCAP...02..036L

[15] R. Durrer and A. Neronov, "Cosmological magnetic fields: their generation, evolution and observation," *Astronomy and Astrophysics Review*, vol. 21, p. 62, Jun. 2013. http://adsabs.harvard.edu/abs/2013A%26ARv..21...62D

[16] K. Freese, J. A. Frieman, and A. V. Olinto, "Natural inflation with pseudo Nambu-Goldstone bosons," *Physical Review Letters*, vol. 65, pp. 3233–3236, Dec. 1990. http://adsabs.harvard.edu/abs/1990PhRvL..65.3233F

[17] J. A. Frieman, C. T. Hill, A. Stebbins, and I. Waga, "Cosmology with Ultralight Pseudo Nambu-Goldstone Bosons," *Physical Review Letters*, vol. 75, pp. 2077–2080, Sep. 1995. http://adsabs.harvard.edu/abs/1995PhRvL..75.2077F

[18] S. M. Carroll, "Quintessence and the Rest of the World: Suppressing Long-Range Interactions," *Physical Review Letters*, vol. 81, pp. 3067–3070, Oct. 1998. http://adsabs.harvard.edu/abs/1998PhRvL..81.3067C

[19] N. Kaloper and L. Sorbo, "Of pNGB quiScript Ntessence," *JCAP*, vol. 4, p. 007, Apr. 2006. http://adsabs.harvard.edu/abs/2006JCAP...04..007K

[20] C. R. Contaldi, J. Magueijo, and L. Smolin, "Anomalous Cosmic-Microwave-Background Polarization and Gravitational Chirality," *Phys. Rev. Lett.*, vol. 101, p. 141101, Oct. 2008. https://ui.adsabs.harvard.edu/#abs/2008PhRvL.101n1101C

[21] V. Gluscevic and M. Kamionkowski, "Testing parity-violating mechanisms with cosmic microwave background experiments," *Phys. Rev. D.*, vol. 81, no. 12, p. 123529, Jun. 2010. http://adsabs.harvard.edu/abs/2010PhRvD..81l3529G

[22] D. Harari and P. Sikivie, "Effects of a Nambu-Goldstone boson on the polarization of radio galaxies and the cosmic microwave background," *Physics Letters B*, vol. 289, pp. 67–72, Sep. 1992. http://adsabs.harvard.edu/abs/1992PhLB..289...67H

[23] S. M. Carroll, G. B. Field, and R. Jackiw, "Limits on a Lorentz- and parity-violating modification of electrodynamics," *Phys. Rev. D.*, vol. 41, pp. 1231–1240, Feb. 1990. http://adsabs.harvard.edu/abs/1990PhRvD..41.1231C

[24] S. Hanany, M. Alvarez, E. Artis *et al.*, "PICO: Probe of Inflation and Cosmic Origins," *arXiv e-prints*, Feb. 2019. https://ui.adsabs.harvard.edu/abs/2019arXiv190210541H

[25] J.-B. Melin, J. G. Bartlett, Z.-Y. Cai, G. De Zotti, J. Delabrouille, M. Roman, and A. Bonaldi, "Dust in galaxy clusters: Modeling at millimeter wavelengths and impact on Planck cluster cosmology," *Astron. Astrophys.*, vol. 617, p. A75, Sep. 2018.

[26] Y. B. Zeldovich and R. A. Sunyaev, "The Interaction of Matter and Radiation in a Hot-Model Universe," *ApSS*, vol. 4, pp. 301–316, Jul. 1969. http://adsabs.harvard.edu/abs/1969Ap%26SS...4..301Z

[27] R. A. Sunyaev and Y. B. Zeldovich, "The Observations of Relic Radiation as a Test of the Nature of X-Ray Radiation from the Clusters of Galaxies," *Comments on Astrophysics and Space Physics*, vol. 4, p. 173, Nov. 1972. http://adsabs.harvard.edu/abs/1972CoASP...4..173S

[28] B. T. Draine and A. A. Fraisse, "Polarized Far-Infrared and Submillimeter Emission from Interstellar Dust," *Ap. J.*, vol. 696, pp. 1–11, May 2009. http://adsabs.harvard.edu/abs/2009ApJ...696....1D

[29] V. Guillet, L. Fanciullo, L. Verstraete *et al.*, "Dust models compatible with Planck intensity and polarization data in translucent lines of sight," *Astron. Astrophys.*, vol. 610, p. A16, Feb. 2018. http://adsabs.harvard.edu/abs/2018A%26A...610A..16G

[30] B. T. Draine and B. Hensley, "Magnetic Nanoparticles in the Interstellar Medium: Emission Spectrum and Polarization," *Ap. J.*, vol. 765, p. 159, Mar. 2013. http://adsabs.harvard.edu/abs/2013ApJ...765..159D

[31] Planck Collaboration, R. Adam, P. A. R. Ade *et al.*, "Planck intermediate results. XXX. The angular power spectrum of polarized dust emission at intermediate and high Galactic latitudes," *Astron. Astrophys.*, vol. 586, p. A133, Feb. 2016. http://adsabs.harvard.edu/abs/2016A%26A...586A.133P

[32] H. K. Eriksen, J. B. Jewell, C. Dickinson, A. J. Banday, K. M. Górski, and C. R. Lawrence, "Joint Bayesian Component Separation and CMB Power Spectrum Estimation," *Ap. J.*, vol. 676, pp. 10–32, Mar. 2008. http://adsabs.harvard.edu/abs/2008ApJ...676...10E

[33] PICO website, "Simulating dipole calibration for PICO." https://sites.google.com/umn.edu/picomission/home/simulating_dipole_pico

[34] A. Suzuki, K. Arnold, J. Edwards *et al.*, "Multi-Chroic Dual-Polarization Bolometric Detectors for Studies of the Cosmic Microwave Background," *Journal of Low Temperature Physics*, vol. 176, pp. 650–656, Sep. 2014. https://ui.adsabs.harvard.edu/#abs/2014JLTP..176..650S

[35] R. O'Brient, P. Ade, K. Arnold *et al.*, "A dual-polarized broadband planar antenna and channelizing filter bank for millimeter wavelengths," *Applied Physics Letters*, vol. 102, p. 063506, Feb. 2013. https://ui.adsabs.harvard.edu/#abs/2013ApPhL.102f3506O

[36] E. D. Shirokoff, "The South Pole Telescope bolometer array and the measurement of secondary Cosmic Microwave Background anisotropy at small angular scales," Ph.D. dissertation, University of California, Berkeley, Jan. 2011. https://ui.adsabs.harvard.edu/#abs/2011PhDT.....383S

[37] L. Bleem, P. Ade, K. Aird *et al.*, "An Overview of the SPTpol Experiment," *Journal of Low Temperature Physics*, vol. 167, pp. 859–864, Jun. 2012. https://ui.adsabs.harvard.edu/#abs/2012JLTP..167..859B

[38] A. D. Turner, J. J. Bock, J. W. Beeman *et al.*, "Silicon nitride Micromesh Bolometer Array for Submillimeter Astrophysics," *Appl. Optics*, vol. 40, pp. 4921–4932, Oct. 2001. https://ui.adsabs.harvard.edu/#abs/2001ApOpt..40.4921T

[39] PICO website, "Q/U Pixel Layout for PICO." https://sites.google.com/umn.edu/picomission/home/qu_pixels

[40] H. Hui, P. A. R. Ade, Z. Ahmed *et al.*, "BICEP Array: a multi-frequency degree-scale CMB polarimeter," in *Society of Photo-Optical Instrumentation Engineers (SPIE) Conference Series*, vol. 10708, Jul. 2018, p. 1070807. https://ui.adsabs.harvard.edu/#abs/2018SPIE10708E..07H

[41] M. C. Runyan, P. A. R. Ade, M. Amiri *et al.*, "Design and performance of the SPIDER instrument," in *Millimeter, Submillimeter, and Far-Infrared Detectors and Instrumentation for Astronomy V*, vol. 7741, Jul. 2010, p. 77411O. https://ui.adsabs.harvard.edu/#abs/2010SPIE.7741E..1OR

[42] P. J. Shirron, M. O. Kimball, D. J. Fixsen, A. J. Kogut, X. Li, and M. J. DiPirro, "Design of the PIXIE adiabatic demagnetization refrigerators," *Cryogenics*, vol. 52, pp. 140–144, Apr. 2012. https://ui.adsabs.harvard.edu/#abs/2012Cryo...52..140S

[43] P. J. Shirron, M. O. Kimball, B. L. James *et al.*, "Thermodynamic performance of the 3-stage ADR for the Astro-H Soft-X-ray Spectrometer instrument," *Cryogenics*, vol. 74, pp. 24–30, Mar. 2016. https://ui.adsabs.harvard.edu/#abs/2016Cryo...74...24S

[44] D. Durand, R. Colbert, C. Jaco, M. Michaelian, T. Nguyen, M. Petach, and J. Raab, "Mid Infrared Instrument (miri) Cooler Subsystem Prototype Demonstration," in *Advances in Cryogenic Engineering*, ser. American Institute of Physics Conference Series, J. G. Weisend, J. Barclay, S. Breon *et al.*, Eds., vol. 52, Mar. 2008, pp. 807–814. https://ui.adsabs.harvard.edu/#abs/2008AIPC..985..807D

[45] J. Rabb et al, "Ngas scw-4k," Presentation at the 2013 Space Cryogenics Workshop, 2013.

[46] D. S. Glaister, W. Gully, R. Ross, P. Hendershott, E. Marquardt, and V. Kotsubo, "Ball Aerospace 4-6 K Space Cryocooler," in *Advances in Cryogenic Engineering: Transactions of the Cryogenic Engineering Conference*, ser. American Institute of Physics Conference Series, I. Weisend, J. G., J. Barclay, S. Breon *et al.*, Eds., vol. 823, Apr. 2006, pp. 632–639. https://ui.adsabs.harvard.edu/#abs/2006AIPC..823..632G

[47] F. Pajot, P. A. R. Ade, J. L. Beney *et al.*, "Planck pre-launch status: HFI ground calibration," *Astron. Astrophys.*, vol. 520, p. A10, Sep. 2010. https://ui.adsabs.harvard.edu/#abs/2010A&A...520A..10P

[48] C. L. Bennett, M. Bay, M. Halpern *et al.*, "The Microwave Anisotropy Probe Mission," *Ap. J.*, vol. 583, pp. 1–23, Jan. 2003. https://ui.adsabs.harvard.edu/#abs/2003ApJ...583....1B

[49] J. A. Tauber, N. Mandolesi, J. L. Puget *et al.*, "Planck pre-launch status: The Planck mission," *Astron. Astrophys.*, vol. 520, p. A1, Sep. 2010. https://ui.adsabs.harvard.edu/#abs/2010A&A...520A...1T

[50] D. Dutcher, P. A. R. Ade, Z. Ahmed *et al.*, "Characterization and performance of the second-year SPT-3G focal plane," in *Society of Photo-Optical Instrumentation Engineers (SPIE) Conference Series*, vol. 10708, Jul. 2018, p. 107081Z. https://ui.adsabs.harvard.edu/#abs/2018SPIE10708E..1ZD

[51] Y. Li, J. E. Austermann, J. A. Beall *et al.*, "Performance of the advanced ACTPol low frequency array," in *Society of Photo-Optical Instrumentation Engineers (SPIE) Conference Series*, vol. 10708, Jul. 2018, p. 107080A. https://ui.adsabs.harvard.edu/#abs/2018SPIE10708E..0AL

[52] BICEP2 and Keck Array Collaborations, P. A. R. Ade, Z. Ahmed *et al.*, "BICEP2 / Keck Array X: Constraints on Primordial Gravitational Waves using Planck, WMAP, and New BICEP2/Keck Observations through the 2015 Season," *arXiv e-prints*, Oct. 2018. http://adsabs.harvard.edu/abs/2018arXiv181005216A

[53] B. Westbrook, A. Cukierman, A. Lee, A. Suzuki, C. Raum, and W. Holzapfel, "Development of the Next Generation of Multi-chroic Antenna-Coupled Transition Edge Sensor Detectors for CMB Polarimetry," *Journal of Low Temperature Physics*, vol. 184, pp. 74–81, Jul. 2016. https://ui.adsabs.harvard.edu/#abs/2016JLTP..184...74W

[54] S. M. Simon, J. E. Golec, A. Ali *et al.*, "Feedhorn development and scalability for Simons Observatory and beyond," in *Society of Photo-Optical Instrumentation Engineers (SPIE) Conference Series*, vol. 10708, Jul. 2018, p. 107084B. https://ui.adsabs.harvard.edu/#abs/2018SPIE10708E..4BS

[55] A. S. Rahlin, P. A. R. Ade, M. Amiri *et al.*, "Pre-flight integration and characterization of the SPIDER balloon-borne telescope," in *Millimeter, Submillimeter, and Far-Infrared Detectors and Instrumentation for Astronomy VII*, vol. 9153, Jul. 2014, p. 915313. https://ui.adsabs.harvard.edu/#abs/2014SPIE.9153E..13R

[56] M. Ferlet, G. Laurent, B. Swinyard, J. Glenn, J. Bock, and K. Dohlen, "Characterisation of Herschel-SPIRE flight model optical performances," in *Space Telescopes and Instrumentation 2008: Optical, Infrared, and Millimeter*, ser. Society of Photo-Optical Instrumentation Engineers (SPIE) Conference Series, vol. 7010, Jul. 2008, p. 70102U. https://ui.adsabs.harvard.edu/#abs/2008SPIE.7010E..2UF

[57] J. T. Sayre, P. Ade, K. A. Aird *et al.*, "Design and characterization of 90 GHz feedhorn-coupled TES polarimeter pixels in the SPTPol camera," in *Millimeter, Submillimeter, and Far-Infrared Detectors and Instrumentation for*

Astronomy VI, vol. 8452, Sep. 2012, p. 845239. https://ui.adsabs.harvard.edu/#abs/2012SPIE.8452E..39S

[58] PICO website, "PICO: Probe of Inflation and Cosmic Origins." https://sites.google.com/umn.edu/picomission

[59] J. Mrozinski and M. DiNicola, "NICM: Cryocooler," NASA 2017 Cost Symposium Presentations, August 2017. https://www.nasa.gov/offices/ocfo/cost_symposium/2017_presentations

[60] P. Gloesener, "Large Aluminium Convex Mirror for the Cryo-Optical Test of the Planck Primary Reflector," in *ESA Special Publication*, vol. 621, Jun. 2006, p. 43. https://ui.adsabs.harvard.edu/#abs/2006ESASP.621E..43G

[61] Y. Toulemont, T. Passvogel, G. Pillbrat, D. de Chambure, D. Pierot, and D. Castel, "The 3.5m all SiC telescope for Herschel," in *5th International Conference on Space Optics*, B. Warmbein, Ed., vol. 554, Jun. 2004, pp. 341–348. https://ui.adsabs.harvard.edu/#abs/2004ESASP.554..341T

[62] S. Bard, "Development of a High-Performance Cryogenic Radiator with V-Groove Radiation Shields," *Journal of Spacecraft and Rockets*, vol. 24, pp. 193–197, May 1987. https://ui.adsabs.harvard.edu/#abs/1987JSpRo..24..193B